Image Compression and Retrieval Techniques for Multi-Application Smart Card

[1]L.M. PALANIVELU and [2]Dr. P. VIJAYA KUMAR, M.E. PhD

[1] Associate Professor - CSE department, Velalar College of Engineering & Technology, Erode, India
E-mail: vcet.lmp@gmail.com
[2] Department of EEE, Karpagam College of Engineering, Coimbatore, India

Abstract: Smart cards future is based on its ability to contain data in its memory and perform operations like comparing data with external databases, computing of digital signatures from other data and including multiple applications. Smart cards should be able to store images like photos, biometric and medical images required for varied applications. Thus, images in the smart card are compressed. This study focuses on the image retrieval problem using compressed images and the impact of compression in the classification accuracy. In this paper, we investigate lossy compression techniques required for various images in multi-application smart card framework and classification accuracy for retrieving compressed image. The images are decomposed using Symlet wavelets. In this work, we propose to compress images including photo of the smart card holder, biometric information and medical images using Embedded Zero trees of Wavelets (EZW) algorithm. Features from the image are extracted using Gabor filters. The classification accuracy for retrieval of uncompressed images and various compressed images is evaluated using Naïve Bayes.

[L.M. PALANIVELU and P. VIJAYA KUMAR. **Image Compression and Retrieval Techniques for Multi-Application Smart Card.** *Life Sci J* 2013;10(4s):531-541] (ISSN: 1097-8135). http://www.lifesciencesite.com. 81

Keywords: Smart Card, Image Compression, Symlet Wavelet, Gabor filters, Embedded Zero trees of Wavelets (EZW)

1. Introduction

Smart cards future is based on its ability to contain data in its memory and perform operations like comparing data with external databases, computing of digital signatures from other data and including multiple applications. Privacy, security and authentication have important roles in multi-application smart cards which should be capable of storing and retrieving data with security so that they cannot be accessed from outside the card, but only through software on the card [1]. This thereby ensures that they are good for security purposes like protecting encrypted files confidentiality or providing transaction proof. Smart cards are the best tool when when authentication is required for identification [2].

The major drawback in the multi-application smart card is the limited and expensive storage medium built into it. With secure online databases becoming popular, storage problems are mitigated to some extent by identifying data sought and controlling access to it through use of pointers to a database record and also identifying user category and their rights to view or change data. This is important. For example, in a driving license, its validity and history of offences might be sought by one group whereas revoking the license or recording offences might be handled by another department. In health records systems, similarly, various health professionals will have different needs/rights to view patient records while patient privacy is crucial and should be protected [3].

France's Carte Vitale card ensures controlled access to medical records stored centrally or in a distributed environment and records access needs both the patient's and health professional's cards – the access level granted depends on the professional's qualifications and specialization; Malaysian government multipurpose smartcard (called MyKad) is an implementation of the national identity card (NIC) and driving license (DL) applications into a smart card. W. H. Loo et al., undertook a study to discover user acceptance of MyKad applications with recommendations to increase acceptance rates and resolving discovered issues [4].

Toji et al., proposed a network based platform for multi-application smart cards used for various business entities on an open network [5]. Markantonakis et al., studied whether smart card technology in banking could be used, not only to combat fraud, but also to achieve a competitive advantage without traditional IT system drawbacks [6]. Multi-application smart card authentication is proposed through integrating handwritten and digital signatures into a public key infrastructure [7].

Signal analysis, image processing and data compression use wavelets which sort out scale information, while maintaining a degree of time/space locality. They also decompose images and store image information. Time-scale wavelets are appropriate to analyse fractal fields as structure functions are obtained through scaling and translating one or two "mother functions". Wavelets analyse

non-stationary time series, whereas Fourier analysis is usually not [9]. A signal's wavelet transform provides its time-frequency representation without changing its information content.

This study focuses on image retrieval issues using compressed images and compression impact in classification accuracy. This paper investigates lossy compression techniques of various images in multi-application smart card framework and classification accuracy in compressed image retrieval. Images are decomposed using Symlet wavelets. Investigations find the appropriate Symlet wavelet (Symlet 2, Symlet 4, Symlet 6 and Symlet 8) and decomposition level (2, 3) for effective compression ratio and PSNR value. In this work, we propose to compress images including photo of the smart card holder, biometric information and medical images using Embedded Zero trees of Wavelets (EZW) algorithm. Image features are extracted using Gabor filters. Classification accuracy of uncompressed image retrieval and various compressed images are evaluated using Naïve Bayes. Medical image compression's aim is performance of medical image matching from an online server containing high resolution images.

2. Methodology

2.1 Symlet Wavelet for Decomposition

Wavelet is a time and frequency bounded waveform. Fourier analysis includes breaking up a signal into sine waves of varied frequency. Similarly, wavelet analysis is breaking up of a signal into shifted and scaled versions of original or mother wavelet. The continuous wavelet transform (CWT) is the sum of all signal time multiplied by scaled, shifted versions of wavelet function ψ.

Mathematically, the continuous wavelet is defined by

$$C(scale, position) = \int_{-\infty}^{\infty} f(t)\psi(scale, position, t)dt$$

CWT results in many wavelet coefficients C, a function of scale and position. Multiplying each coefficient by appropriately scaled and shifted wavelet yields the original signal's constituent wavelets.

Symlets are nearly symmetrical wavelets proposed by Daubechies as modifications to the db family with the properties of both wavelet families being similar [10, 11]. . Symlets are compactly supported wavelets with least asymmetry and highest number of vanishing moments for a given support width [12].

2.2 Embedded Zero trees of Wavelets (EZW) for Compression

Embedded bit stream is a desirable property for image compression schemes [13, 14]. When encoded as an embedded bit stream, an image suits progressive transmission, where the entire image is always visible becoming clearer as received. This contrasts raster-based transmission where an image is transmitted row-by-row, completely decompressed, with only a portion of the image being visible until completely received [13, 15]. The Embedded Zero trees of Wavelets (EZW) algorithm produces an embedded bit stream from an image transformed into the frequency domain using DWT. The EZW algorithm generated bit stream represents a sequence of binary decisions distinguishing an image from the null or gray image. This allows an encoder to terminate encoding at any time, allowing a target bit rate to be reached correctly. Similarly, a decoder can terminate decoding any time, allowing progressive transmission.

Wavelets algorithms embedded zerotrees processes hierarchical wavelet decomposition of images. EZW exploits image self-similarity inherent by introducing a data structure called zero tree [16]. the idea being that if a coefficient at a coarse scale is insignificant regarding a given threshold, then all wavelet coefficients of similar orientation in the same spatial location at finer scales are also likely to be insignificant. Figure 1 reveals the zerotree structure where each coefficient has four descendants at a finer scale, except the coarsest scale, the LL sub band, having three descendants for every coefficient [17].

To perform the embedded coding, an initial threshold is chosen

$$t_0 = 2^{(\log_2(max|h(x,y)|))}$$

where h(x, y) denotes a coefficient. The encoder alternates between the dominant and the subordinate pass till the image is completely encoded or desired bit rate achieved. A dominant pass is followed by a subordinate pass where the next most significant bit of coefficients in subordinate list is outputted. In other words, first T is subtracted from a coefficient. Then T/2 becomes the subordinate threshold. If the coefficient is greater than or equal to T/2, then a '1' is outputted, otherwise a '0' is outputted.

Following subordinate pass, threshold is halved (T = T/2), and another dominant pass started, this cycle continuing till the threshold T = 0, or the encoder halts the process as the target bit rate was achieved. The image is converted to the YUV colour scheme for colour images. An initial threshold was chosen with the largest value in Y band. A dominant pass is performed on every separate band in the

image, the Y, U, and V bands. Then subordinate pass is performed on all values in the subordinate list.

2.3 Gabor Filter for feature extraction

Gabor filters frequency and orientation representations are similar to that of the human visual system, and are appropriate for texture representation and discrimination [18, 19]. A 2D Gabor filter is a Gaussian kernel function modulated by a sinusoidal plane wave in the spatial domain. Gabor filters are self-similar: all filters being generated from one mother wavelet by dilation/rotation.

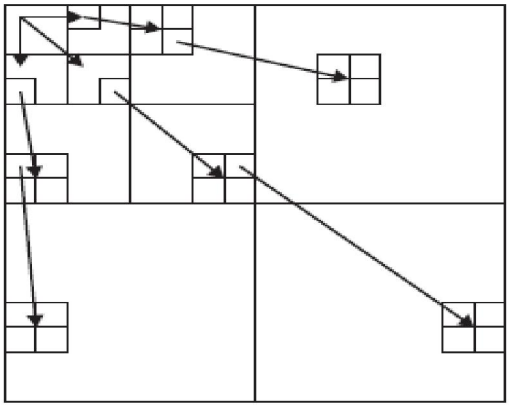

Figure 1: Zerotree structure of EZW algorithm

The one-dimensional Gabor filter is defined as the Multiplication of a cosine/sine (even/odd) wave with Gaussian windows as follows [20],

$$G_E(X) = \frac{1}{\sqrt{2\pi\sigma^2}} e^{\frac{-x}{2\sigma^2}} \cos(2\pi w_0 x)$$

$$G_0(X) = \frac{1}{\sqrt{2\pi\sigma^2}} e^{\frac{-x}{2\sigma^2}} \sin(2\pi w_0 x)$$

Where w_0 defines the centre frequency (i.e., the frequency in which the filter yields the greatest response) and σ the spread of the Gaussian window.

Texture is important in image analysis for classification/segmentation and image generation, computer vision, graphics and image processing. Currently many texture feature extraction algorithms have been developed which are helpful for surface inspection in industry and also tissue characterization in medicine. Though textures in real world are coloured, image processing research focused on gray scale textures, the reason being high colour camera cost, high computational cost of colour image processing and complexity of colour textures. Figure 2 reveals the flowchart for Gabor filter feature extraction. Gray scale texture features are subdivided into statistical and signal theoretic algorithms, the classes being selected based on underlying stochastic process or a specific Fourier pattern, respectively. Prominent representatives for statistical texture feature extraction methods include Gauss-Markov random fields [21] and Co-occurrence matrices [22]. Gabor and wavelet representations are based on a windowed Fourier transform.

3. Results and Discussion

In this work, MRI image, passport photograph of card holder and fingerprint images obtained from FVC2006 competition were used to evaluate the proposed method. 50 images of Passport photograph, 50 images of fingerprint and 50 MRI images of which 20 were stroke images and 30 non-stroke images were used for decompressing, compression and classification. Some of the images used are shown in Figure 3.

The steps followed are summarized below:

1. Images were decomposed using Symlet 2, Symlet 4, Symlet 6 for decomposition level 2, 3.
2. Compress images including photo of the smart card holder, biometric information and medical images using Embedded Zero trees of Wavelets (EZW) algorithm. Number of pass used in EZW- 5, 10, 15.
3. The classification accuracy for retrieval of uncompressed images and various compressed images is evaluated using k Nearest Neighbor.

The following parameters are determined to evaluate the efficiency of compression of the techniques.

Compression Ratio: The compression performance is evaluated using compression ratio (CR). It is the ration of the size of the compressed file over the size of the original file, given as,

Compression Factor is given by

$$CR(\%) = \frac{\text{bytes of compressed signal}}{\text{bytes of original signal}} X\ 100$$

CF = 100/Compression ratio

Two of the error metrics used to compare the various image compression techniques are Mean Square Error (MSE) and Peak Signal to Noise Ratio (PSNR).

Mean Square Error (MSE): MSE is the cumulative squared error between compressed and original image, while PSNR is a measure of peak error. A lower MSE value means lesser error, and as seen from the inverse relation between MSE and PSNR, it translates to a high PSNR value. Logically, a higher PSNR value is good as it means the ratio of Signal to Noise is higher. Here, the 'signal' is the original image, and 'noise' the reconstruction error. The mathematical formulae for the two are

$$MSE = \frac{1}{MN} \sum_{y=1}^{M} \sum_{x=1}^{N} \left[I(x,y) - I'(x,y) \right]^2$$

$$PSNR = 20 * Log10\left(255 / \sqrt{MSE}\right)$$

where I(x,y) is the original image, I'(x,y) is the

approximated version (which is actually the decompressed image) and M,N are the dimensions of the images.

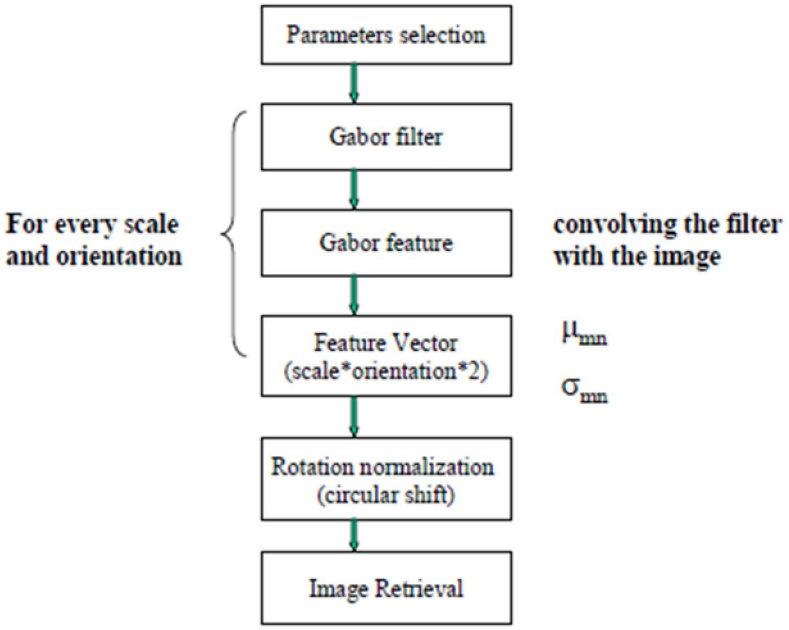

Figure 2: Feature Extraction Using Gabor Filter

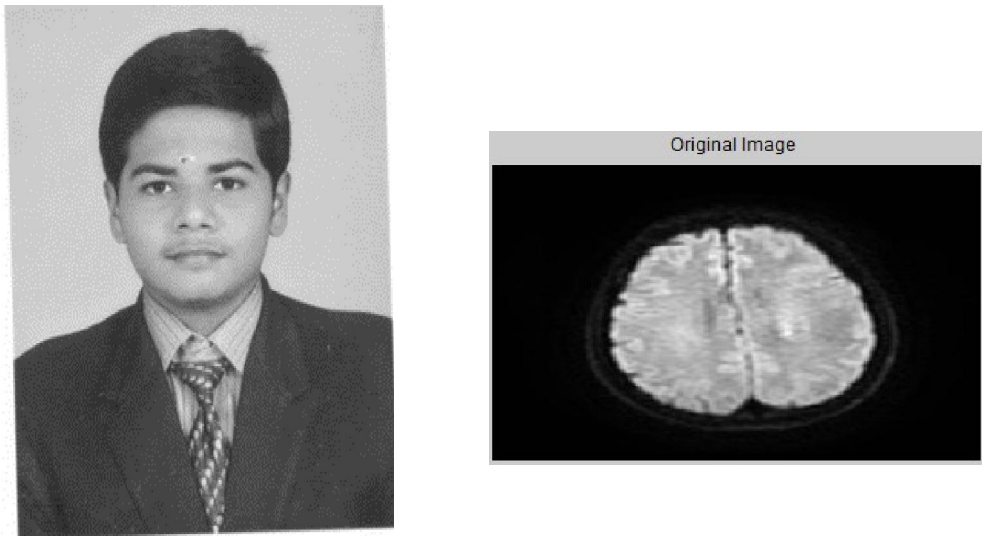

Figure 3: Different images used in the experimental setup

3.1 Results of Decomposition and Compression

Table 1 show the results in terms of compression ratio and PSNR for Symlet 2, decomposition level 2 and EZW compression for the passport photograph. Figure 4 shows the graph of the same.

Table 1: Compression Ratio and PSNR for the Passport Photograph using Symlet 2, Decomposition level: 2, EZW compression

Photo	CR	PSNR	Photo	CR	PSNR
PP01	21.13	39.38	PP26	23.88	38.92
PP02	20.13	39.3	PP27	32.75	39.4
PP03	30.38	39.16	PP28	24.25	39.08
PP04	27.75	38.89	PP29	24.88	39.55
PP05	18.63	39.43	PP30	20.63	39.47
PP06	31.5	39.63	PP31	23.13	39.31
PP07	25.88	38.78	PP32	23	38.88
PP08	26.38	39.21	PP33	31.5	39.01
PP09	27.25	39.67	PP34	22	39.63
PP10	29.5	39.29	PP35	22.88	39.5
PP11	30.88	38.96	PP36	24.38	38.92
PP12	24	38.95	PP37	28.75	39.45
PP13	19.63	38.95	PP38	20.5	39.23
Photo	CR	PSNR	Photo	CR	PSNR
PP14	29.13	39.29	PP39	31.13	39.37
PP15	23.25	38.9	PP40	19.63	38.88
PP16	30.63	38.93	PP41	25.13	38.84
PP17	23.75	38.88	PP42	18.88	38.97
PP18	30.5	39.38	PP43	29.38	39.1
PP19	21	38.95	PP44	28.63	39.06
PP20	20.25	39.39	PP45	21.5	38.88
PP21	31.25	39.46	PP46	28.38	39.56
PP22	19	39.35	PP47	26.5	38.96
PP23	28.38	38.91	PP48	24.72	39.34
PP24	29.13	39.22	PP49	23.68	39.52
PP25	24.75	39.65	PP50	27.48	39.31

It is seen that an average compression ratio of 25.43 is achieved for the photographs varying from 18.88 to 32.75. Similarly, the average achieved for PSNR is 39.2 varying from 38.84 to 39.67. The performance of PSNR is more consistent.

Figure 5 show the results in terms of compression ratio and PSNR for Symlet 2, decomposition level 2 and EZW compression for the fingerprint.

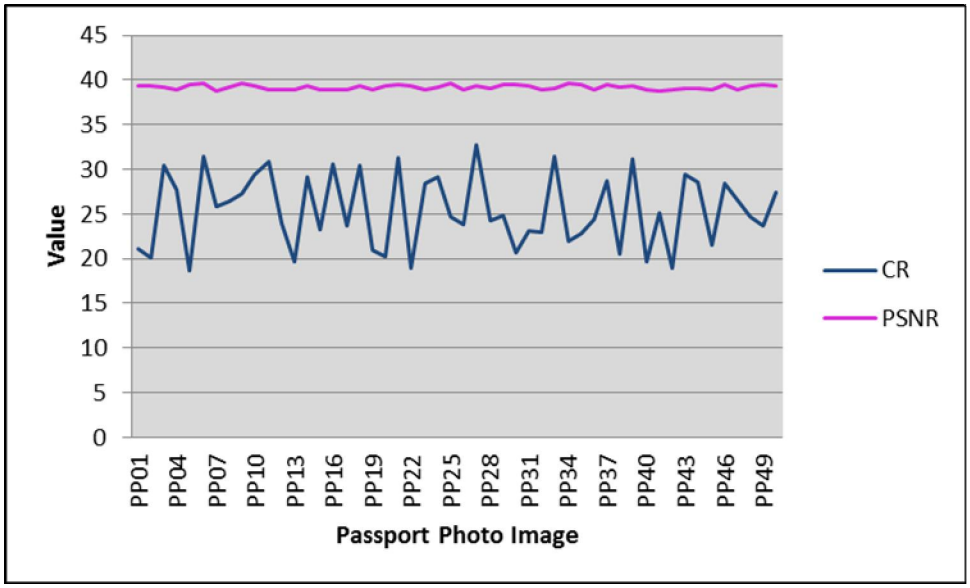

Figure 4: Compression Ratio and PSNR for the Passport Photograph using Symlet 2, Decomposition level: 2, EZW compression

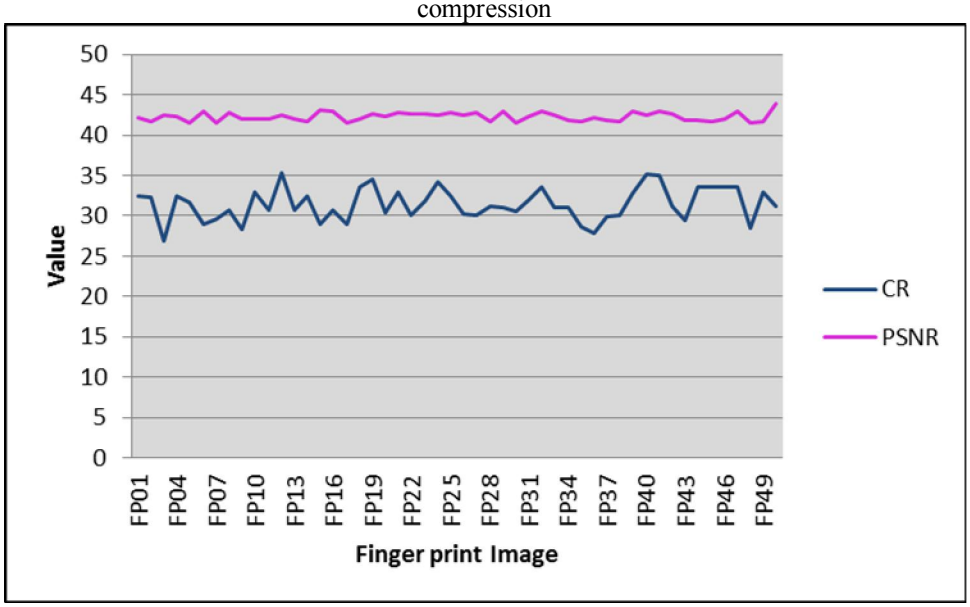

Figure 5: Compression Ratio and PSNR for the Fingerprint using Symlet 2, Decomposition level: 2, EZW compression

It is seen that an average compression ratio of 31.43 is achieved for the photographs varying from 26.88 to 34.13. Similarly, the average achieved for PSNR is 42.28 varying from 41.5 to 43.95. The performance of PSNR is more consistent and the compression ratio is higher than that achieved for photograph.

Figure 6 show the results in terms of compression ratio and PSNR for Symlet 2, decomposition level 2 and EZW compression for the Medical images. It is seen that an average compression ratio of 34.62 is achieved for the photographs varying from 31.75 to 37.63. Similarly, the average achieved for PSNR is 44.04 varying from 43.46 to 44.65. The performance of PSNR is more consistent and the compression ratio and PSNR is higher than that achieved for photograph and fingerprint.

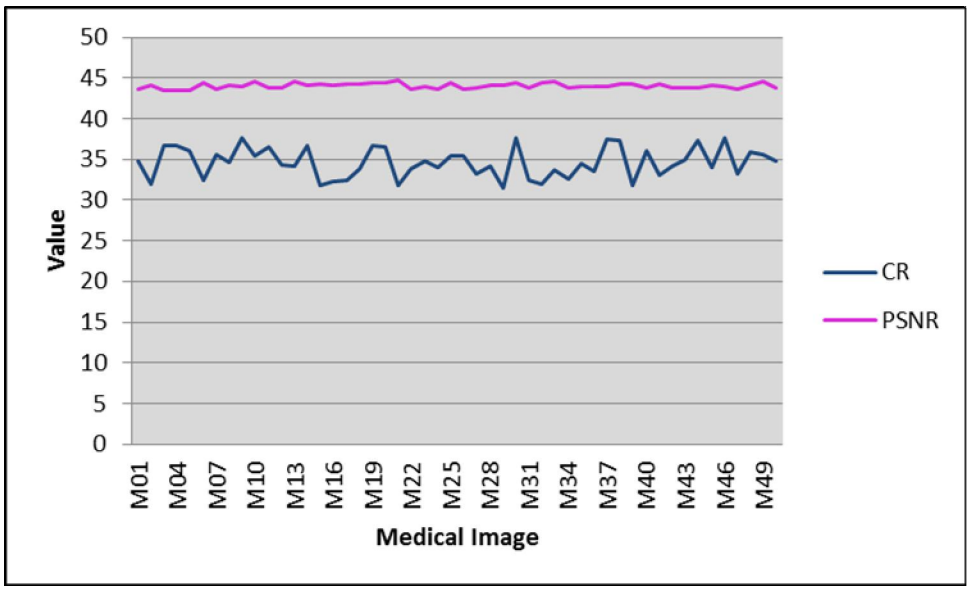

Figure 6: Compression Ratio and PSNR for the Medical Images using Symlet 2, Decomposition level: 2, EZW compression

Figure 7 shows the average compression ratio obtained for Symlet 2, Symlet 4, and Symlet 6 for decomposition level 2 and decomposition level 3 for all images. Figure 8 shows the average PSNR obtained for Symlet 2, Symlet 4, and Symlet 6 for decomposition level 2 and decomposition level 3 for photo, fingerprint and medical image.

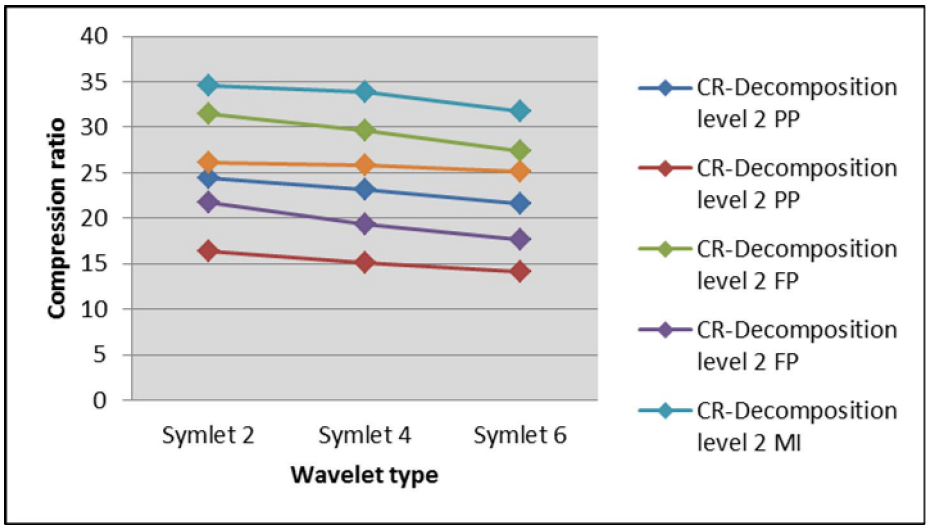

Figure 7: Average compression ratio obtained for Symlet 2, Symlet 4, and Symlet 6 for decomposition level 2 and decomposition level 3.

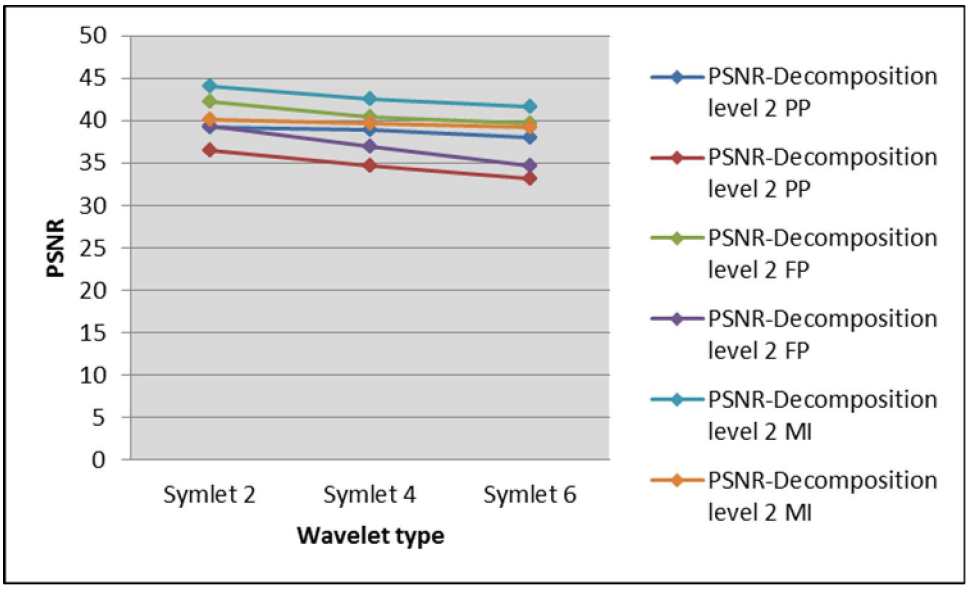

Figure 8: Average PSNR obtained for Symlet 2, Symlet 4, and Symlet 6 for decomposition level 2 and decomposition level 3.

It is observed from the graphs that the compression ratio and PSNR is high for Symlet 2 at decomposition level 2.

The following Figures show the original and decomposed images for photo.

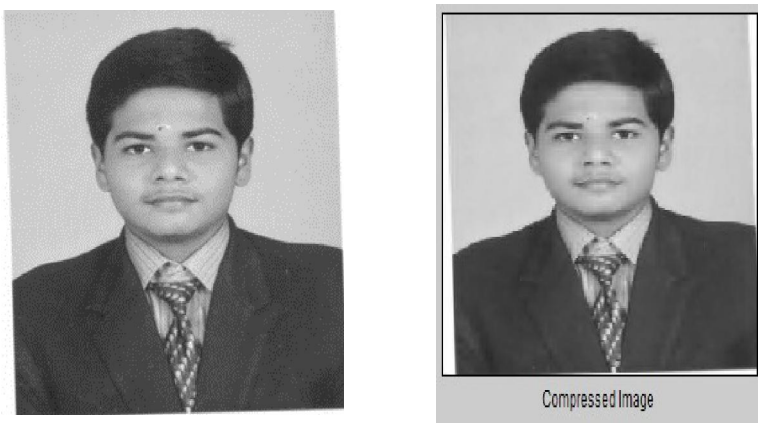

Figure 9: a. The Original Photo; b. The Compressed Photo

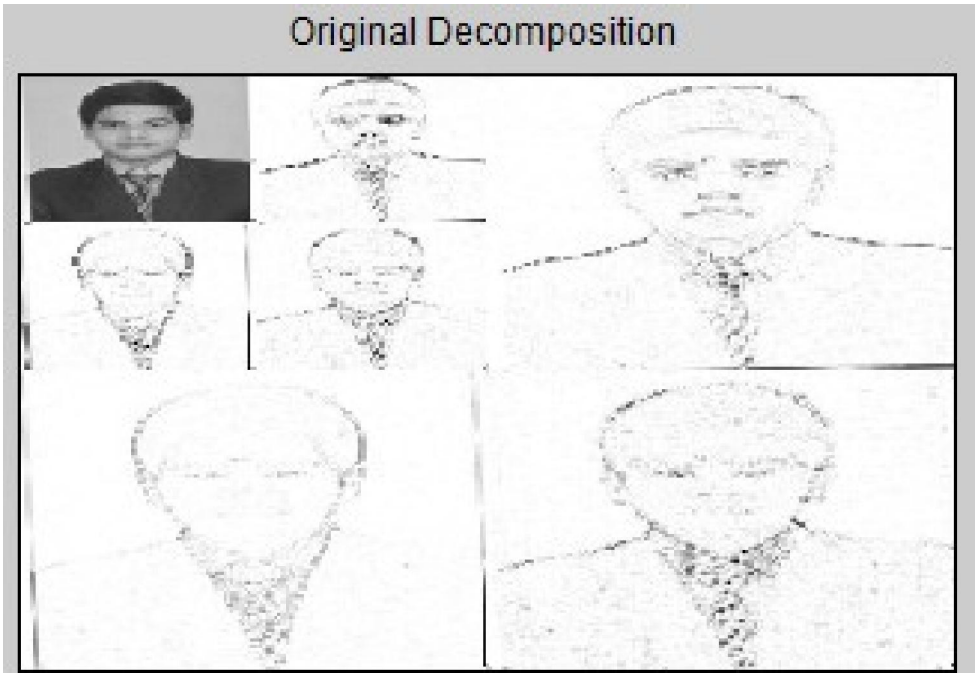

Figure 10: The Compressed Photo and the two level decomposition

Table 2 tabulates the average obtained for Symlet 2, Symlet 4, and Symlet 6 for decomposition level 2 and decomposition level 3.

Table 2: Average obtained for Symlet 2, Symlet 4, and Symlet 6 for decomposition level 2 and decomposition level 3.

	Passport photo			
	Decomposition level 2		Decomposition level 3	
	CR-Decomposition level 2 PP	PSNR-Decomposition level 2 PP	CR-Decomposition level 2 PP	PSNR-Decomposition level 2 PP
Symlet 2	24.36	39.2	16.42	36.45
Symlet 4	23.16	38.89	15.16	34.68
Symlet 6	21.62	37.95	14.08	33.17
	Fingerprint			
	Decomposition level 2		Decomposition level 3	
	CR-Decomposition level 2 FP	PSNR-Decomposition level 2 FP	CR-Decomposition level 2 FP	PSNR-Decomposition level 2 FP
Symlet 2	31.43	42.28	21.68	39.28
Symlet 4	29.62	40.36	19.38	36.87
Symlet 6	27.41	39.65	17.68	34.69
	Medical Image			
	Decomposition level 2		Decomposition level 3	
	CR-Decomposition level 2 MI	PSNR-Decomposition level 2 MI	CR-Decomposition level 2 MI	PSNR-Decomposition level 2 MI
Symlet 2	34.62	44.04	26.17	40.06
Symlet 4	33.88	42.48	25.89	39.68
Symlet 6	31.82	41.67	25.12	39.24

4.2 Classification Accuracy Results

Figure 11 shows the classification accuracy obtained for Symlet 2, Symlet 4, and Symlet 6 for decomposition level 2 and decomposition level 3 for all images. Table 3 tabulates the same.

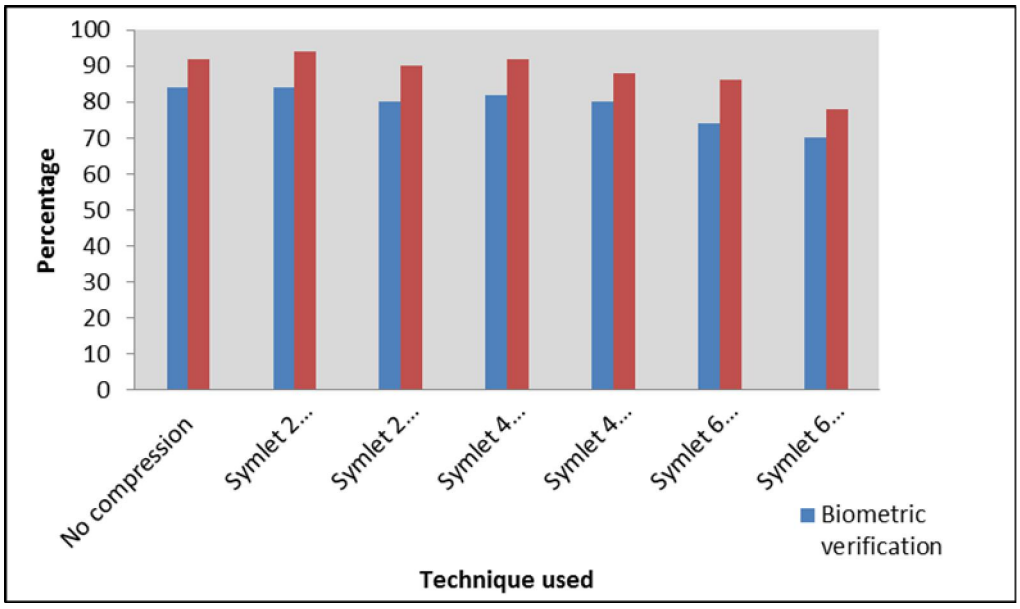

Figure 3.11: Classification Accuracy obtained for Symlet 2, Symlet 4, and Symlet 6 for decomposition level 2 and decomposition level 3 for all images.

Table 3: Classification Accuracy obtained for Symlet 2, Symlet 4, and Symlet 6 for decomposition level 2 and decomposition level 3 for all images.

Classification accuracy	Biometric verification	Stroke classification
No compression	84	92
Symlet 2 Decomposition 2	**84**	**94**
Symlet 2 Decomposition 3	80	90
Symlet 4 Decomposition 2	82	92
Symlet 4 Decomposition 3	80	88
Symlet 6 Decomposition 2	74	86
Symlet 6 Decomposition 3	70	78

It is observed that the classification accuracy achieved for the compressed images is similar to or better when compared to the accuracy of uncompressed images.

4. Conclusion

In this paper, investigations are carried out to evaluate compression techniques required for various images in multi-application smart card framework and classification accuracy for retrieving compressed image. This study focuses on the image retrieval problem using compressed images and the impact of compression in the classification accuracy. The ultimate goal of medical image compression is to perform medical image matching from an online server containing high resolution images. Experiments were conducted using 50 images of Passport photograph, 50 images of fingerprint and 50 MRI images of which 20 were stroke images and 30 non-stroke images. The images are decomposed using Symlet wavelets and Embedded Zero trees of Wavelets (EZW) algorithm was used for compressing the images. Features from the image are extracted using Gabor filters. The classification accuracy for retrieval of uncompressed images and various compressed images is evaluated using k Nearest Neighbor. Experimental results revealed that the best compression ratio and PSNR is achieved for Symlet 2 at decomposition level 2. Similarly, it is observed that the classification accuracy achieved for the compressed images is similar to or better when compared to the accuracy of uncompressed images when the images are decomposed using Symlet 2 at decomposition level 2.

References

[1] Xu, J., Zhu, W. T., & Feng, D. G. (2009). An improved smart card based password authentication scheme with provable security. Computer Standards & Interfaces, 31(4), 723-728.

[2] Hendry, M. (2007). Multi-application smart cards: technology and applications. Cambridge university press.

[3] Hsu, M. H., Yen, J. C., Chiu, W. T., Tsai, S. L., Liu, C. T., & Li, Y. C. (2011). Using health smart cards to check drug allergy history: The

perspective from Taiwan's experiences. Journal of medical systems, 35(4), 555-558.
[4] Loo, W. H., Yeow, P. H., & Chong, S. C. (2009). User acceptance of Malaysian government multipurpose smartcard applications. Government Information Quarterly, 26(2), 358-367.
[5] Toji, R., Wada, Y., Hirata, S., & Suzuki, K. (2001). A network-based platform for multi-application smart cards. In Enterprise Distributed Object Computing Conference, 2001. EDOC'01. Proceedings. Fifth IEEE International (pp. 34-45). IEEE.
[6] Markantonakis, K. (2008). Multi Application Smart Card Platforms and Operating Systems. Smart Cards, Tokens, Security and Applications, 51-83.
[7] Elfadil, N. A., & Al-raisi, Y. J. (2008, May). An approach for multi factor authentication for securing smart cards' applications. In Computer and Communication Engineering, 2008. ICCCE 2008. International Conference on(pp. 368-372). IEEE.
[8] Wakin, M. B. (2011). Sparse Image and Signal Processing: Wavelets, Curvelets, Morphological Diversity (Starck, J.-L., et al; 2010)[Book Reviews]. Signal Processing Magazine, IEEE, 28(5), 144-146.
[9] Manimaran, P., Panigrahi, P. K., & Parikh, J. C. (2009). Multiresolution analysis of fluctuations in non-stationary time series through discrete wavelets.Physica A: Statistical Mechanics and its Applications, 388(12), 2306-2314.
[10] D.L. Donoho, "De-noising by soft thresholding", IEEE Trans. Trans. Inform. Theory, vol. 41, pp. 613-627, 1995
[11] Reddy, G. U., Muralidhar, M., & Varadarajan, S. (2009). ECG De-Noising using improved thresholding based on Wavelet transforms. IJCSNS, 9(9), 221.
[12] Ahmed, S., Ahmad, S., Faruqe, M. O., & Islam, M. R. (2009, November). EMG signal decomposition using wavelet transformation with respect to different wavelet and a comparative study. In Proceedings of the 2nd International Conference on Interaction Sciences: Information Technology, Culture and Human (pp. 730-735). ACM.
[13] Shapiro, J. M. (1993). Embedded image coding using zerotrees of wavelet coefficients. Signal Processing, IEEE Transactions on, 41(12), 3445-3462.
[14] Shukla, J., Alwani, M., & Tiwari, A. K. (2010, April). A survey on lossless image compression methods. In Computer Engineering and Technology (ICCET), 2010 2nd International Conference on (Vol. 6, pp. V6-136). IEEE.
[15] Usevitch, B. E. (2001). A tutorial on modern lossy wavelet image compression: foundations of JPEG 2000. Signal Processing Magazine, IEEE, 18(5), 22-35.
[16] Shapiro, J. M. (1992, March). An embedded wavelet hierarchical image coder. In Acoustics, Speech, and Signal Processing, 1992. ICASSP-92., 1992 IEEE International Conference on (Vol. 4, pp. 657-660). IEEE.
[17] Bhattar, R. K., Ramakrishnan, K. R., & Dasgupta, K. S. (2002). Strip based coding for large images using wavelets. Signal Processing: Image Communication, 17(6), 441-456.
[18] Field, D. J., Hayes, A., & Hess, R. F. (1993). Contour integration by the human visual system: Evidence for a local "association field". Vision research, 33(2), 173-193.
[19] Fogel, I., & Sagi, D. (1989). Gabor filters as texture discriminator. Biological cybernetics, 61(2), 103-113.
[20] Daugman, J. G. (1985). Uncertainty relation for resolution in space, spatial frequency, and orientation optimized by two-dimensional visual cortical filters. Optical Society of America, Journal, A: Optics and Image Science, 2, 1160-1169.
[21] Mahmoodi, S., & Gunn, S. (2011, September). Snake based unsupervised texture segmentation using Gaussian Markov random field models. In Image Processing (ICIP), 2011 18th IEEE International Conference on (pp. 3353-3356). IEEE.
[22] Kekre, H. B., & Gharge, S. (2009, January). SAR Image Segmentation using co-occurrence matrix and slope magnitude. In Proceedings of the International Conference on Advances in Computing, Communication and Control (pp. 368-372). ACM.

2/26/2013